J|A|C|S
ARTICLES
Published on Web 06/14/2007

Phase-Controlled Growth of Metastable Fe_5Si_3 Nanowires by a Vapor Transport Method

Kumar S. K. Varadwaj,[†] Kwanyong Seo,[†] Juneho In,[†] Paritosh Mohanty,[†] Jeunghee Park,[‡] and Bongsoo Kim*[,†]

Contribution from the Department of Chemistry, KAIST, Daejeon 305-701, Korea, and Department of Chemistry, Korea University, Jochiwon 339-700, Korea

Received March 4, 2007; E-mail: bongsoo@kaist.ac.kr

Abstract: We report the synthesis of single-crystalline nanowires (NWs) of metastable Fe_5Si_3 phase via an iodide vapor transport method. Free-standing Fe_5Si_3 NWs are grown on a sapphire substrate placed on a Si wafer without the use of any catalyst. The typical size of the Fe_5Si_3 nanowires is 5−15 μm in length and 100−300 nm in diameter. Synthesis of the metastable phase is induced by composition-dependent nucleation from the gas-phase reaction. Depending on the concentration ratio of FeI_2(g) to SiI_4(g), different phases of iron silicides are formed. The growth of nanowires is facilitated by the initial nucleation of silicide particles on the substrate and further self-seeded growth of the NWs. The present work not only provides a method for the synthesis of metastable Fe_5Si_3 nanowires but also suggests that the phase controlled synthesis can be further optimized to produce other metal-rich silicide nanostructures for future spintronic devices.

Introduction

Iron and silicon in their solid-solution series produce a rich variety of binary compounds with a wide range of magnetic, electrical, and optical properties.[1] FeSi has attracted much attention because of its anomalous temperature-dependent electrical, optical, and magnetic properties, similar to those of Kondo insulators.[2] Co substitution for Fe in FeSi, moreover, produces unusual positive magnetoresistance and a large anomalous Hall Effect, making $Fe_{1-x}Co_xSi$ a potential candidate for spintronics applications.[3] The silicon-rich phase in the solid-solution series such as β-$FeSi_2$ is a direct band gap material and can be used as a light emitting diode (LED) in silicon.[4] Ferromagnetic properties are observed in iron-rich phases such as Fe_3Si and Fe_5Si_3.[5] Fe_5Si_3 is a high-temperature phase, which is metastable with respect to a mixture of FeSi and Fe_3Si below 825 °C.[6] Fe_5Si_3 has a Curie temperature of 110 °C and giant magnetoresistance (GMR) has been observed in nanogranular Fe_5Si_3 in a silicon matrix.[5]

The traditional solid-state reactions involve the mixing of bulk reactant solids and annealing at elevated temperatures. The mechanisms of these reactions are primarily based on three steps: interdiffusion of the reactant elements in solid state, nucleation, and growth of the crystalline product. High temperature and long reaction time are necessary to overcome the high activation energies for long-range diffusion in extended solids.[6] In these diffusion-limited solid-state reactions, only thermodynamically stable phases in the phase diagram nucleate. The vapor deposition method has been shown to be a potentially effective approach to synthesize metastable solids. Jansen et al. synthesized metastable solids by a vapor deposition method in which the desired components undergo atomic level mixing on the substrate and react at very mild temperatures to form metastable solids.[7] This method circumvents the high activation energy necessary for transport in the bulk materials and leads to the formation of metastable materials. A few approaches to synthesize metastable phases in the solid state have also been reported. The Fe_5Si_3 phase which is stable at high temperature in bulk can be formed by rapid cooling of the melt.[5b] T. Novet et al. developed a method for the synthesis of Fe_5Si_3 thin films in which the ultrathin amorphous elemental layers diffuse at a low temperature and nucleation becomes the rate-determining step in the formation of crystalline materials.[6] Using this approach they demonstrated composition dependent crystalline

[†] KAIST.
[‡] Korea University.

(1) Massalski, T. B. *Binary Alloy Phase Diagrams*; American Society for Metals: Ohio, 1986; Vol. 1, p 1100.
(2) (a) Paschen, S.; Felder, E.; Chernikov, M. A.; Degiorgi, L.; Schwer, H.; Ott, H. R.; Young, D. P.; Sarrao, J. L.; Fisk, Z. *Phy. Rev. B* **1997**, *56*, 12916. (b) Aeppli, G.; Fisk, Z. *Comments Condens. Matter Phys.* **1992**, *16*, 155. (c) Schlesinger, Z.; Fisk, Z.; Zhang, H. -T.; Maple, M. B.; DiTusa, J. F.; Aeppli, G. *Phys. Rev. Lett.* **1993**, *71*, 1748. (d) Sluchanko, N. E.; Glushkov, V. V.; Demishev, S. V.; Menovsky, A. A.; Weckhuysen, L.; Moshchalkov, V. V. *Phys. Rev. B* **2002**, *65*, 064404.
(3) (a) Manyala, N.; Sidis, Y.; DiTusa, J. F.; Aeppli, G.; Young, D. P.; Fisk. Z. *Nature* **2000**, *404*, 581. (b) Manyala, N.; Sidis, Y.; DiTusa, J. F.; Aeppli, G.; Young, D. P.; Fisk, Z. *Nat. Mater.* **2004**, *3*, 255.
(4) Leong, D.; Harry, M.; Reeson, K. J.; Homewood, K. P. *Nature* **1997**, *387*, 686.
(5) (a) Hines, W. A.; Menotti, A. H.; Budnick, J. I.; Burch, T. J.; Litrenta, T.; Niculescu, V.; Raj, K. *Phys. Rev. B* **1976**, *13*, 4060. (b) Lecocq, Y.; Lecocq, P.; Michel, A. *C. R. Acad. Sci.* **1964**, *258*, 5655. (c) Sawatzky, E. *IEEE Trans. Magn.* **1971**, 374. (d) Srivastava, P. C.; Tripathi, J. K. *J. Phys. D: Appl. Phys.* **2006**, *39*, 1465.
(6) Novet, T.; Johnson, D. C. *J. Am. Chem. Soc.* **1991**, *113*, 3398.
(7) Jansen, M. *Angew. Chem., Int. Ed.* **2002**, *41*, 3746 and references therein.

10.1021/ja071439v CCC: $37.00

phase nucleation in a Fe−Si system, by which Fe_5Si_3 phase is formed at a low temperature.

Nanowires (NWs) often show distinct properties from their bulk counterparts because of radial confinement.[8,9] Since metal silicide NWs can be used as interconnects in integrated circuits and they are compatible with the processing of complementary metal-oxide-semiconductor (CMOS) devices,[10] the synthesis of metal silicide NWs has been extensively studied recently. Growth of self-assembled rare earth silicide NWs from the anisotropic lattice mismatch between the NW and the silicon substrate has been reported.[11] It has been demonstrated that the growth of $CoSi_2$ and $FeSi_2$ NWs is induced by endotaxial growth into the substrate.[12] For bottom-up device applications, nevertheless, there is continuing research to develop synthetic methods for freestanding silicide NWs. Freestanding NiSi NWs can be prepared by the initial deposition of Ni on single crystalline Si NWs followed by annealing and etching of the extra metal.[10b,13] Schmitt et al. reported on the synthesis of freestanding FeSi NWs based on an organometallic single source precursor.[14] FeSi NWs are also formed by evaporating $FeCl_3$ onto silicon substrates at a high temperature via a method developed by Ouyang et al.[15] In both methods only NWs of FeSi phase are formed. This is due to the use of a single source precursor in the first case and thermodynamic preference of the FeSi phase to other iron silicide phases in the second case. Herein we report on a vapor transport based method for the synthesis of metastable Fe_5Si_3 NWs. Development of new synthetic strategies to form iron silicide NWs with iron-rich compositions may help to realize NWs with ferromagnetic property, which are important for future spintronic devices. To the best of our knowledge, there has been no report on the synthesis of freestanding Fe_5Si_3 NWs in the vapor phase.

Experimental Section

Single crystalline Fe_5Si_3 NWs were synthesized in a horizontal hot-wall two-zone furnace with a 1 in. diameter inner quartz tube, as shown in Scheme 1. The setup is equipped with pressure and mass flow controllers. The synthetic approach is based on a simple modification of the van-Arkel method,[16] in which the the exothermic reaction of metal and iodine is used to transport the metal from a mixture by halide formation. The metal vapor redeposits reversibly at higher temperatures. We have modified the process for the synthesis of silicide NWs: The

Scheme 1. Experimental Setup

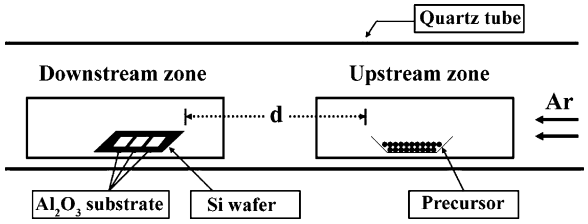

FeI_2 precursor is evaporated at a low temperature and transported to the high-temperature zone by carrier gas, where Fe is deposited after the dissociation of FeI_2 on the preheated substrate. The upstream (US) zone and downstream (DS) zone were used for vaporization of precursor and NW growth, respectively. A rectangular Si wafer (45 mm length and 15 mm width) kept at the DS zone was the source of Si. The silicide NWs were grown on c-plane sapphire substrates placed on the Si wafer. This scheme helps to control the Si composition in the NW. Anhydrous FeI_2 powder (50 mg from Sigma-Aldrich, 99.999%) in an alumina boat was placed at the center of the US zone. The system was purged with Ar gas for 30 min before the start of each reaction to maintain an inert atmosphere. The flow rate of carrier Ar was varied between 100 and 250 sccm to synthesize silicide NWs of different phases. The substrates were placed at ∼10 cm (*d* value in Scheme 1) from the precursor position in the DS zone. The DS zone was initially heated to 900 °C. After reaching the target temperature, the temperature of the US zone was raised to 500 °C at a heating rate of 40 °C /min. The reaction time was varied between 5 and 30 min.

The X-ray diffraction (XRD) pattern of the as grown NW ensemble was recorded on a Rigaku D/max-rc (12 kW) diffractometer operated at 40 kV voltage and 80 mA current with filtered 0.15405 nm Cu Kα radiation. Field emission scanning electron microscope (FESEM) images of the NWs were taken on a Phillips XL30S. Transmission electron microscope (TEM) images, high-resolution TEM (HRTEM) images, and selected area electron diffraction (SAED) patterns were taken on JEOL JEM-2100F TEM operated at 200 kV. Chemical compositions of the NWs were studied by X-ray energy-dispersive spectrometry (EDS) attached to the TEM. The samples for TEM analysis were prepared either by dispersing the NWs in solvent followed by placing a drop of the solution on a carbon coated copper grid or by dragging the grids along the surface of the sample.

Results and Discussion

A. Synthesis and Characterization of Fe_5Si_3 NWs. The NWs of metastable Fe_5Si_3 phase are synthesized from the FeI_2 precursor on a sapphire substrate placed on top of a Si wafer. The representative SEM images in Figure 1 a,b show the morphology of the NWs. Investigation by SEM and TEM images (Figure 2) reveals that the NW diameters range from 100 to 300 nm and the lengths vary from 5 to 15 micrometers. Figure 1c shows the XRD pattern from the as grown NWs ensemble, in which all the diffraction peaks are indexed to the hexagonal Fe_5Si_3 structure (JCPDS file: 11-0615). The highest intensity peak corresponding to the Fe_5Si_3 (212) plane is at an identical position to that of the FeSi (210) plane. However, the (104), (300), and (114) peaks in the pattern clearly show that the NWs are composed of crystalline Fe_5Si_3. The TEM image from a representative NW in Figure 2a shows that the NW is made up of a 100 nm diameter silicide core covered with a modulated silica layer. The SAED pattern of the NW shows a regular spot pattern, reflecting the single-crystalline nature of the NWs. The diffraction pattern is fully indexed to the hexagonal Fe_5Si_3 structure and shows that the NW has [001] growth direction. The SAED patterns obtained from other NWs

(8) (a) Xia, Y.; Yang, P.; Sun, Y.; Wu, Y.; Mayers, B.; Gates, B.; Yin, Y.; Kim, F.; Yan, H. *Adv. Mater* **2003**, *15*, 353. (b) Cui, Y.; Lieber, C. M. *Science* **2001**, *291*, 851. (c) Huang, M. H.; Mao, S.; Feick, H.; Yan, H.; Wu, Y.; Kind, H.; Weber, E.; Russo, R.; Yang, P. *Science* **2001**, *292*, 1897. (d) Wang, Z. L.; Song, J. *Science* **2006**, *312*, 242. (e) Chan, C. K.; Peng, H.; Twesten, R. D.; Jarausch, K.; Zhang, X. F.; Cui, Y. *Nano Lett.* **2007**, *7*, 490.
(9) Jung, Y.; Lee, S.-H.; Ko, D.-K.; Agarwal, R. *J. Am. Chem. Soc.* **2006**, *128*, 14026.
(10) (a) Chueh, Y.-L.; Ko, M.-T.; Chou, L.-J.; Chen, L.-J.; Wu, C.-S.; Chen, C.-D. *Nano Lett.* **2006**, *6*, 1637. (b) Wu, Y.; Xiang, J.; Yang, C.; Lu, W.; Lieber, C. M. *Nature* **2004**, *430*, 61. (c) Zhang, S. L.; Ostling, M. *Crit. Rev. Solid State Mater Sci.* **2003**, *28*, 1.
(11) (a) Chen, Y.; Ohlberg, D. A. A.; Williams, R. S. *J. Appl. Phys.* **2002**, *91*, 3213. (b) Nogami, J.; Liu, B. Z.; Katkov, M. V.; Ohbuchi, C.; Birge, N. O. *Phys. Rev. B* **2001**, *63*, 233305. (c) Liu, B. Z.; Nogami, J. *J. Appl. Phys.* **2003**, *93*, 593. (d) Preinesberger, C.; Becker, S. K.; Vandre, S.; Kalka, T.; Dahne, M. *J. Appl. Phys.* **2002**, *91*, 1695.
(12) (a) He, Z.; Smith, D. J.; Bennet, P. A. *Phys. Rev. Lett.* **2004**, *93*, 256102. (b) Liang, S.; Islam, R.; Smith, D. J.; Bennett, P. A.; O'Brien, J. R.; Taylor, B.; *Appl. Phys. Lett.* **2006**, *88*, 113111.
(13) Decker, C. A.; Solanki, R.; Freeouf, J. L.; Carruthers, J. R.; Evans, E. R. *Appl. Phys. Lett.* **2004**, *84*, 1389.
(14) Schmitt, A. L.; Bierman, M. J.; Schmeisser, D.; Himpsel, F. J.; Jin, S. *Nano Lett.* **2006**, *6*, 1617.
(15) Ouyang, L.; Thrall, E. S.; Deshmukh, M. M.; Park, H. *Adv. Mater* **2006**, *18*, 1437.
(16) van Arkel, A. E.; de Boer, J. H. *Z. Anorg. Allg. Chem.* **1925**, *148*, 345.

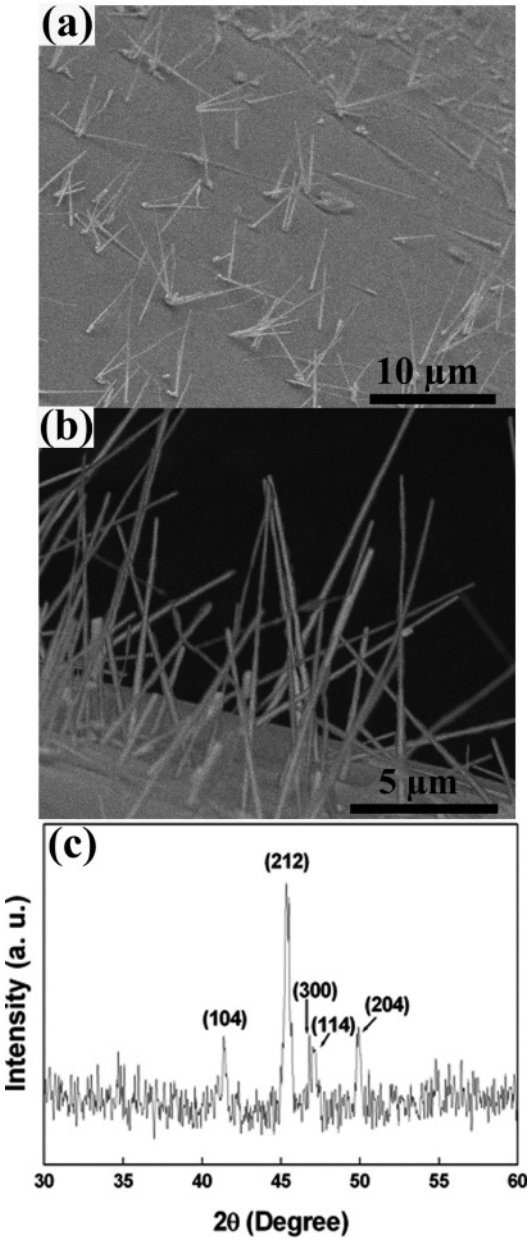

Figure 1. (a) Representative SEM image of Fe_5Si_3 NWs; (b) high magnification SEM image of Fe_5Si_3 NWs; (c) XRD pattern of the Fe_5Si_3 NWs on *c*-plane sapphire substrate.

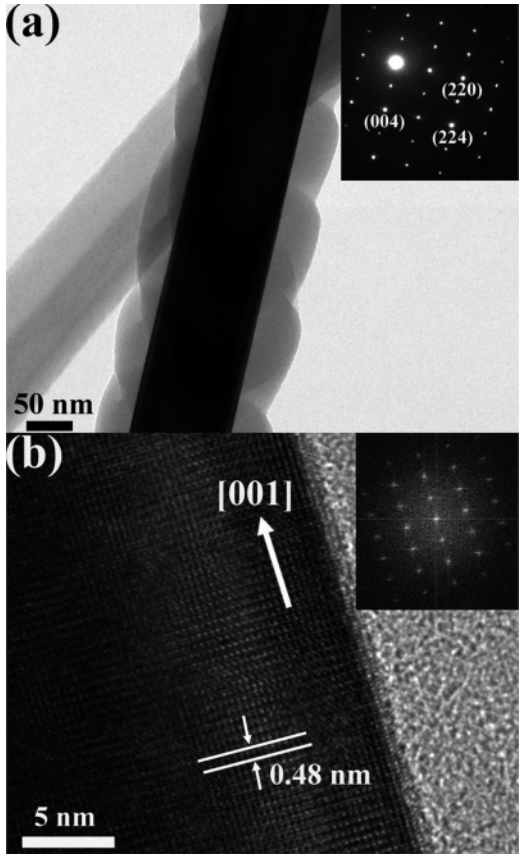

Figure 2. (a) Representative TEM image and SAED pattern. The SAED pattern is indexed for a hexagonal Fe_5Si_3 NW down the [$\bar{1}$10] zone axis. (b) Representative high-resolution TEM image. The labeled distance of 0.48 nm corresponds to the (002) planes, and the arrow shows the [001] growth direction of the NW. The inset in Figure 2b shows the two-dimensional fast Fourier transform (FFT).

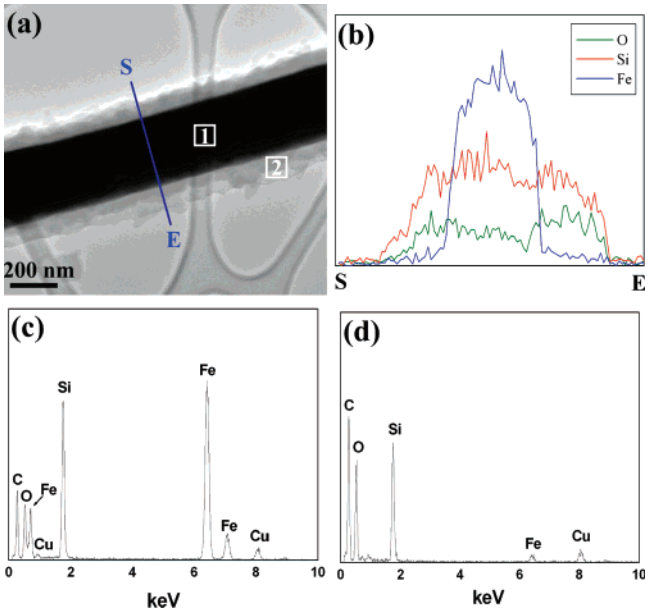

Figure 3. EDS analysis of the Fe_5Si_3 NWs; (a) TEM image of the Fe_5Si_3 NW; (b) EDS line profiles for the Fe_5Si_3 NW from S to E in panel a. (c) EDS spectrum from the center of the NW, area 1 in panel a; (d) EDS spectrum from the NW shell, area 2 in panel a.

are identical. Figure 2b shows an HRTEM image of a NW with clear lattice fringes, which again confirms the single crystalline nature of the NW. The lattice spacing of the planes parallel to the growth direction is calculated to be 0.48 nm, which agrees well with the spacing of the (002) planes of a hexagonal Fe_5Si_3 structure. The two-dimensional fast Fourier transform (FFT) of the lattice resolved image (inset of Figure 2b) obtained from the HRTEM can also be indexed to the hexagonal Fe_5Si_3 structure.

Figure 3 shows the composition line profile along the diameter of a NW and EDS spectra of a single Fe_5Si_3 NW. One EDS spectrum is taken at the center of the NW (Figure 3c) and the other is taken at the amorphous layer of the NW (Figure 3d). The EDS spectrum in Figure 3c shows that Fe and Si are the major elements in the NW with a small amount of oxygen (lines due to Cu and C are from the TEM grid). Figure 3d shows that the amorphous layer is composed of Si and O with an atomic ratio close to 1:1. The composition of Fe and Si in the NW core is found to be approximately 5:3 after taking into account

Table 1. The Growth of FeSi and Fe_5Si_3 NWs at Different Reaction Conditions and on Different Substrates

substrate	US temp	DS temp	flow rate	phase formed
sapphire on Si	500 °C	900 °C	200 sccm	Fe_5Si_3 NWs
sapphire on Si	475 °C	900 °C	200 sccm	FeSi NWs
sapphire on Si	500 °C	900 °C	100 sccm	FeSi NWs
Si	500 °C	900 °C	200 sccm	FeSi NWs

the Si concentration due to the oxide layer. The cross-sectional line profile in Figure 3b also shows a uniform composition of Fe and Si along the NW diameter.

B. Phase-Controlled Synthesis of Iron Silicide NWs. Given that a single source organometallic precursor was used in the synthesis of FeSi NWs by Schmitt et al., modification of the precursor would be necessary for further extension of this method to NWs of other iron−silicon binary phases.[14] Ouyang et al. synthesized FeSi NWs using an $FeCl_3$ precursor on a Si substrate.[15] NWs of other iron silicide phases are not obtained by this method. FeSi is the most stable congruently melting compound and has the highest melting point in the Fe−Si binary phase diagram.[17] Therefore, FeSi is the most likely phase to nucleate with the largest free energy gain.

We have achieved the composition tuned synthesis of iron silicide nanowires by growing the NWs on a sapphire substrate placed on a Si wafer. In addition, more flexible control over the reaction conditions is achieved by employing two separate heating zones for precursor evaporation and NW growth (Scheme 1), whereas a single heating zone was used in the method of Ouyang et al. The synthesis conditions for Fe_5Si_3 and FeSi NWs are shown in Table 1. In the synthesis of Fe_5Si_3 NWs, it was found that adoption of a sapphire substrate for NW deposition, while a Si wafer was the source of Si, helped to control the NW composition. When the carrier gas flow rate was reduced to 100 sccm or the US zone temperature was reduced to 475 °C, FeSi NWs were obtained instead of Fe_5Si_3 on the sapphire substrate. This shows that the phase-controlled NW synthesis becomes possible by subtle changes in the reaction conditions, when the sapphire substrate is used for the growth of NWs. We also could get both FeSi and Fe_5Si_3 phases at similar reaction conditions when Si powder packed in an alumina boat was employed as the source of Si instead of a Si wafer, and a sapphire substrate was placed on it for NW growth. For the reaction conditions between those for FeSi and Fe_5Si_3 NWs listed in Table 1 and at distances nearer to the precursors we could see the coexistence of FeSi and Fe_5Si_3 NWs on the same substrate.

When Si substrates were employed alone for NW growth, FeSi was the only iron silicide phase that could be synthesized, which was revealed by various experiments at different reaction conditions.[18] Increasing the iron vapor pressure, however, by raising the precursor evaporation temperature and/or reducing the reaction pressure resulted in secondary growth on the FeSi NW surface producing branches. Further increase of precursor vapor pressure beyond this point produced FeSi microparticles.[18] Notably, when NWs were grown on a sapphire substrate that was placed on a larger Si wafer, either FeSi NWs or microparticles are produced on the uncovered part of the Si wafer, depending on the reaction conditions and the distance from the precursor. No sign of etching or any other structures could be observed on the Si wafer.

The formation of metastable Fe_5Si_3 and FeSi phases may be explained by the following plausible reaction pathways. FeI_2 vapor is transported to the high-temperature (DS) zone and may react directly with the Si substrate in the DS zone to form iron silicide.

$$2FeI_2(g) + 3Si(s) \leftrightarrow 2FeSi(s) + SiI_4(g) \quad \text{[on a Si substrate]} \tag{1}$$

This reaction of the precursor with the Si substrate alone (reaction 1), however, cannot explain the formation of different iron silicide phases on the sapphire substrate. The following two plausible reactions may explain the direct nucleation of different iron silicide phases on the sapphire substrate.

$$5FeI_2(g) + 3SiI_4(g) \leftrightarrow Fe_5Si_3(s) + 11I_2(g) \tag{2}$$

$$FeI_2(g) + SiI_4(g) \leftrightarrow FeSi(s) + 3I_2(g) \tag{3}$$

Interdiffusion of elements is the rate determining step in solid-state reactions between two elements. High temperature and long reaction times allow the nucleation of only a thermodynamically stable binary phase in the phase diagram. In the present synthetic method, reaction 1 is the dominant reaction pathway on the Si substrate. The reaction of precursor vapor with crystalline Si always produces the thermodynamically stable FeSi phase in the Fe−Si binary phase diagram. Therefore, increase in FeI_2 vapor pressure only accelerates the rate of nucleation of the FeSi phase. When the FeI_2 vapor pressure is too high, NW growth is not favored and microparticles are produced.

In principle, vapor transport based reactions can circumvent these limitations of the solid-state reaction as elements undergo atomic level mixing in the vapor phase and nucleation becomes the rate determining step. Thus, the synthesis of several metastable compounds, which would otherwise be inaccessible, such as CoP_2 and tantalates and niobates of thorium, including modifications of Nb_2O_5, has been demonstrated to occur via the vapor-phase reactions.[19] In the present case, we change the iron silicide synthesis conditions and allow the direct nucleation of iron silicides from the vapor phase by placing a sapphire substrate on top of a Si wafer. Then, reactions 2 and 3 can proceed and the undissociated $FeI_2(g)$ reacts with the gaseous Si compound [$SiI_4(g)$]. Since the reaction and mixing of iron and silicon occur in the gas phase, various iron silicide phases can be formed on the sapphire substrate depending on the vapor composition. Control of the $FeI_2(g)$ to $SiI_4(g)$ concentration ratio can be achieved by variation of the FeI_2 vapor pressure, which in turn is determined by the US zone temperature and the carrier gas flow rate. Note that SiI_4 vapor pressure can be also affected by the $FeI_2(g)$ pressure. When the degree of supersaturation is appropriate, composition dependent nucleation of Fe_5Si_3 or FeSi phases occurs on the sapphire substrate.

We further carried out the reaction at low-reaction pressure for faster delivery of the precursor to the growth site. The reaction at 100 Torr produces Fe_5Si_3 nanorods with a hexagonal cross-section (as shown in inset of Figure 4a). The nanorods

(17) Okamoto, H. *Desk Handbook: Phase Diagrams for Binary Alloys*; ASM International: Ohio, 2000.
(18) Supporting Information.
(19) Gruehn, R.; Glaum, R. *Angew. Chem., Int. Ed.* **2000**, *39*, 692 and references therein.

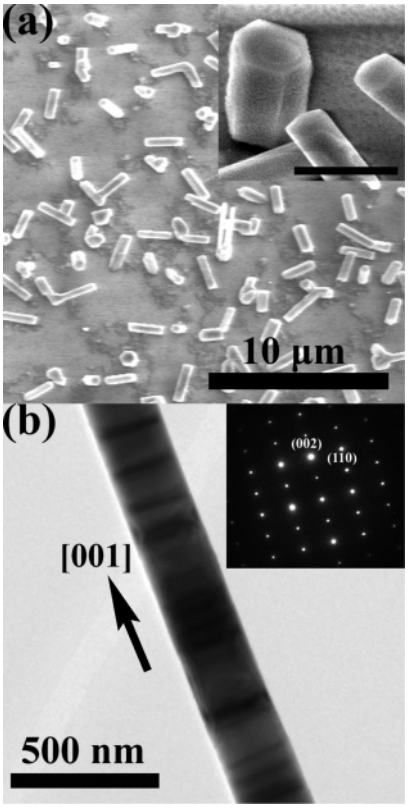

Figure 4. (a) Representative SEM image of Fe_5Si_3 nanorods. The inset shows hexagonal cross-section of the nanorods. Scale bar is 1 μm. (b) Representative TEM image and SAED pattern of Fe_5Si_3 nanorod. The SAED pattern is indexed for a hexagonal Fe_5Si_3 nanorod down the [1$\bar{1}$0] zone axis, which elucidates the single-crystalline nature of the nanorods. The arrow indicates [001] growth direction of the nanorod. No thick silica layer on the surface could be observed in these nanorods.

diameter is about 500 nm and the length is in the range of 2−3 μms. Detailed TEM and SEM analysis did not show any other iron silicide phase on the substrate. These results suggest that lowering the reaction pressure does not alter the composition of FeI_2 and SiI_4 in vapor further. It only increases the degree of supersaturation of Fe_5Si_3, leading to an increase in lateral dimension to produce nanorods.[8a] In the bulk, the high-temperature Fe_5Si_3 phase can be stabilized by rapid cooling from the melt; in the present experiment on the other hand the substrate is slowly cooled inside a furnace. Thus, it appears that the Fe_5Si_3 phase is more stable in the NW or nanorod morphology. The thick silica layer observed on the NW surface (Figure 1b) might not be the driving factor for this higher stability because the Fe_5Si_3 nanorods produced in a slightly different condition do not have a silica layer, but are still found to be equally stable. Thus, it appears that the one-dimensional morphology with [001] growth direction could have produced a low-energy state that improved the stability of this metastable structure. Such a phenomenon was previously observed in the CdSe NWs and ZnS nanobelts, where the one-dimensional nanoform stabilized the metastable phase.[20]

C. Growth Mechanism of Silicide NWs. The possible NW growth mechanism is derived from various experiments conducted in different conditions and from morphology study of the NWs. Because no catalytic metal particles or thin films are employed in the synthesis, vapor−liquid−solid (VLS) growth is unlikely. SEM and TEM studies also do not show the presence of any metal catalyst on the NW tip. Moreover, a detailed EDS study from the tip and the stem of several NWs reveals no significant deviation in the composition of iron and silicon in either Fe_5Si_3 or FeSi NWs. However, when Au nanoparticles are deliberately employed as catalyst on the sapphire substrate, Fe_5Si_3 NWs with radial branches of silica NWs are obtained instead of silicide NWs produced by catalyst assisted growth.[18] To understand the source of oxygen or oxide in these reactions, we etched the native oxide layer on the Si wafer (by 2% HF solution) before the reaction. Although this hindered the growth of uniform silica branches along the silicide NW surface, it did not completely stop the formation of an oxide layer on the silicide NW. This shows that the silica layer is formed during the reaction at high temperature by the oxygen coming from the silica layer on the Si wafer and also from a leakage into the reaction chamber. The nonuniform nature of the oxide shell on the NW surface as shown in Figure 2a, suggests that the oxide layer would not have been formed by the oxidation of silicide NWs in post-growth condition.

The morphology and growth direction of the FeSi NWs synthesized on Si and sapphire substrates are found to be the same (Figure 5a and ref 18). Figure 5 panels c and d show low magnification images of FeSi NWs formed on sapphire and silicon substrates, respectively. Both images show bushlike structures on the substrate, in which each bushy formation is a collection of long NWs. It appears that the growth of Fe_5Si_3 on a sapphire substrate and that of FeSi on both the Si and sapphire substrate proceed in a similar manner. These NW growth processes are apparently initiated by nucleation of silicide particles on the substrate and further self-seeded growth of NWs from the silicide particles.[21,22] It is well-known that Au nanoparticles provide the initial nucleation site for the aligned growth of Si NWs by a VLS mechanism.[23] In the present reaction the Au nanoparticles did not appear to participate in the formation of iron silicide NWs. However, it appears that after the formation of silicide NWs by a self-seeded growth process, Au nanoparticles get attached to a NW surface and form the nucleation site for the growth of silica NWs through a VLS mechanism. The presence of Au nanoparticles on the silica NWs tip supports this conjecture. Notably, in a related reaction for the synthesis of cobalt silicide NWs, we could selectively synthesize CoSi and Co_2Si NWs by systematically changing the reaction conditions and the substrate.[24]

Conclusions

A vapor transport method is developed for the synthesis of single-crystalline NWs of metastable Fe_5Si_3 phase. The NWs are free-standing with an amorphous silica layer covering the silicide core. Phase controlled synthesis of iron silicide NWs is achieved by placing a sapphire substrate on a Si wafer for NW growth and subtle adjustment of the reaction conditions. Various

(20) (a) Wang, Z.; Daemen, L. L.; Zhao, Y.; Zha, C. S.; Downs, R. T.; Wang, X.; Wang, X.; Wang, Z. L.; Hemley, R. J. *Nat. Mater* **2005**, *4*, 922. (b) Zaziski, D.; Prilliman, S.; Scher, E. C.; Casula, M.; Wickham, J.; Clark, S. M.; Alivisatos, A. P. *Nano Lett.* **2004**, *4*, 943.

(21) (a) Wang, Z. L. *Annu. Rev. Phys. Chem.* **2004**, *55*, 159−196. (b) Yang, P. *Mater. Res. Soc. Bull.* **2005**, *30*, 85−91.
(22) Li, Y.; Chang, R. P. H. *J. Am. Chem. Soc.* **2006**, *128*, 12778.
(23) Law, M.; Goldberger, J.; Yang, P. *Annu. Rev. Mater. Res.* **2004**, *34*, 83.
(24) Seo, K, Varadwaj, K. S. K.; Mohanty, P.; Lee, S.; Jo, Y.; Jung, M.-H.; Kim, J.; Kim, B. *Nano Lett.* **2007**, *7*, 1240−1245.

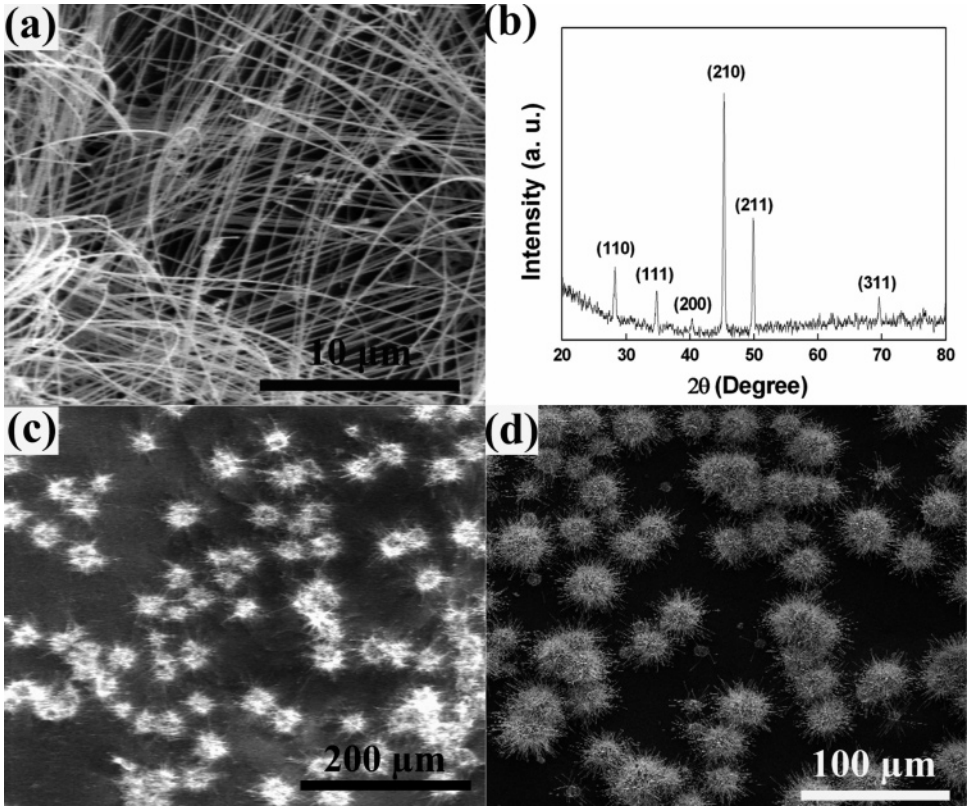

Figure 5. (a) Representative SEM image of FeSi NWs on a *c*-plane sapphire substrate; (b) XRD pattern of FeSi NWs on a *c*-plane sapphire substrate; low-magnification SEM image of FeSi NWs on a (c) *c*-plane sapphire substrate and (d) silicon substrate.

silicide phases are formed on a sapphire substrate by direct vapor-phase reaction of $FeI_2(g)$ and $SiI_4(g)$. We suggest that the process of one-dimensional growth may stabilize the metastable Fe_5Si_3 phase. The growth of the silicide NWs proceeds by nucleation of silicide particles and further growth of NWs from the particles. This simple vapor transport method may be further generalized for the synthesis of other metal silicide NWs with various compositions. These metal-rich ferromagnetic silicide NWs may play an important role in future spintronic applications.

Acknowledgment. This research was supported by a grant-(Code No. 06K1501-02620) from "Center for Nanostructured Materials Technology" under "21st Century Frontier R&D Programs" of the Ministry of Science and Technology, Korea. SEM and TEM analysis was performed at the Korea Basic Science Institute in Daejeon.

Supporting Information Available: FeSi NWs on a Si substrate; FeSi bulk particles on a Si substrate; Fe_5Si_3 NWs with silica branches. This material is available free of charge via the Internet at http://pubs.acs.org.

JA071439V